

Effect of Motor and Propeller Location on the Hover Characteristics of a Single-Blade Rotorcraft

Barathan Jeevaretanam
University of California San Diego, La Jolla, CA, 92092

This study was conducted to gain an understanding into the effects of motor and propeller location on the hover characteristics of a single-blade rotorcraft. The experiment was conducted by first quantifying the relationship between the Electronic Speed Controller (ESC) signal and the angular velocity of the propeller. Then, the motor and propeller were placed at several different locations along the span of the rotorcraft's wing. For each location, throttle joystick data was collected once hover was achieved and then analyzed. The relationship between the ESC signal and the angular velocity of the propeller was found to be linear. The minimum pulse width signal that produced a rotation of the propeller was 1300 μs , while the maximum was 1600 μs . On the other hand, the thrust required to achieve hover decreased as the motor and propeller were moved outwards along the span of the wing. In addition to this, it was found that the propeller was rotating at 76% of its top rotational speed when placed at the outermost location on the wing and at 92% when placed at its innermost location.

Nomenclature

$C_D(\alpha)$	=	Coefficient of drag as a function of angle of attack
$C_L(\alpha)$	=	Coefficient of lift as a function of angle of attack
D	=	Propeller diameter
J	=	Advance ratio
n_{actual}	=	Actual angular velocity
$n_{predicted}$	=	Predicted angular velocity
Q	=	Rotor wing torque
R	=	Location of motor and propeller as measured from the root
T_{AA}	=	Actual thrust produced
T_{AP}	=	Predicted thrust produced
T_{prop}	=	Thrust required for hover
V	=	Airspeed at the propeller location
Ω	=	Wing rotational rate

I. Introduction

A single-blade rotorcraft was designed with the maple seed in mind. The maple seed is able to generate lift by rotating rapidly to slow its decent as it falls. The goal of this project was to build a single-blade rotorcraft that shared similar characteristics to the maple seed. By employing the same technique the maple seed uses, the rotorcraft will instead be made to achieve hover and eventually free flight. The final product is a single-blade rotorcraft consisting of an airfoil, an electronics board, a motor and a propeller. A CAD rendition of the vehicle can be seen in Fig.1.

During the initial building stage of the rotorcraft, the placement of the motor and propeller was decided arbitrarily by the team. After several flight tests, this placement raised a number of questions. It was observed that the placement of the motor and propeller influenced the location of center of gravity of the vehicle, an important parameter in the overall dynamics of the rotorcraft. As a result of this, it was unclear how the performance of the rotorcraft would be affected by the motor and propeller placement. These doubts were the source of motivation behind this experiment. The effect of this placement on the hover characteristics of the rotorcraft was studied to gain a better understanding of this issue. In specific, it was of interest to investigate how the change in location of the motor and propeller along the wingspan would affect the thrust produced to achieve hover. Thus, the objective of this study is to investigate and accurately quantify this relationship. The outcome of this study will allow for more well-informed decision making regarding the placement of the motor and propeller for a given single-blade rotorcraft.

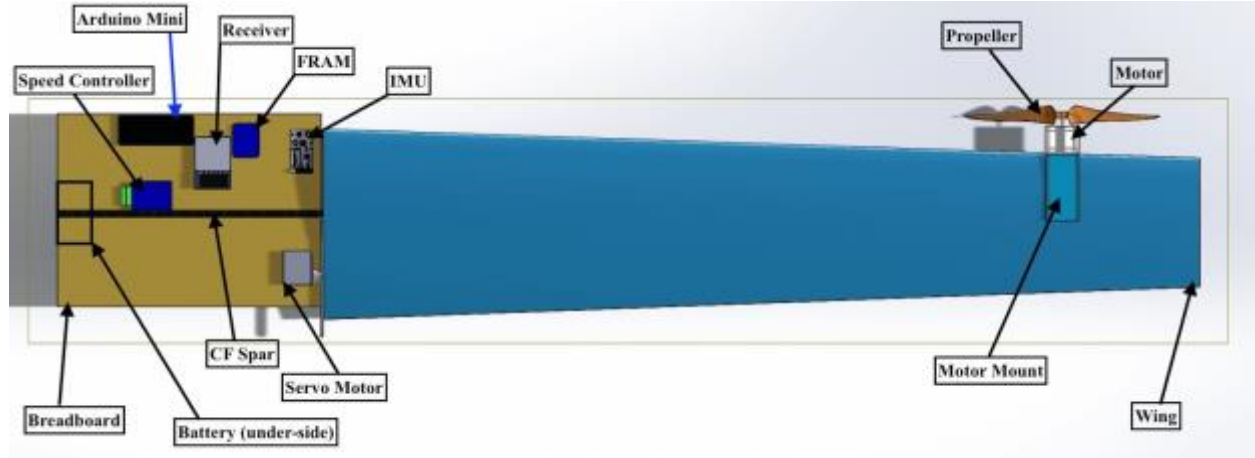


Figure 1. CAD Layout of major structure and components.

II. Procedure

The experiment was conducted in several stages. These separate stages are outlined below:

A. Electronic Speed Controller (ESC) Calibration²

The motor powers the propeller by means of a pulse width signal fed to the ESC. The goal at this stage was to quantify and characterize the relationship between the ESC signal and propeller speed by means of a calibration curve. An Arduino Uno program was written to periodically send a pulse width signal of magnitudes between 1000 μ s and 2000 μ s from the ESC to the motor directly. Each pulse width signal caused the propeller to rotate at some angular velocity. For each pulse width signal sent to the motor from the program, a tachometer was pointed at the propeller and the angular velocity of the propeller was subsequently recorded. This process was first done by increasing the magnitude of the pulse width signal and then once again by decreasing the magnitude from 2000 μ s to 1000 μ s. This was done to mitigate the effects of random errors. Finally, an average angular velocity for each pulse width signal was calculated and a calibration curve was determined.

B. Test Stand Data Collection

The TestSAM program was uploaded onto the electronics board before placing the rotorcraft on the test stand. With power then turned on, the rotorcraft was made to hover using the controller. Once the rotorcraft achieved hover, data collection was begun. In specific, the data that was of interest in this case was the throttle joystick data. The GetSAM program was then used to extract the throttle joystick data obtained during hover. This data contains the magnitude of the pulse width signal that was fed to the motor. The calibration curve was then used to identify the angular velocity of the propeller for that specific pulse width signal. Then, the advance ratio was calculated using the following formula:

$$J = \frac{v}{(n_{actual})D} \quad (1)$$

With the angular velocity and advance ratio now in hand, the propeller data from APC Propellers¹ was used to obtain the thrust produced by the propeller.

C. Varying of Motor and Propeller Location

The motor and propeller was then dismantled and moved to different locations along the wingspan of the rotorcraft (As shown in figures 2a), 2b) and 2c) below). As before, once hover was achieved, data was recorded. The GetSAM program was once again used to extract the pulse width signal that was fed by the ESC to the motor. Then, the same procedure was employed to calculate the advance ratio and eventually the thrust that was produced. A relationship between the location of the motor and propeller, and the thrust produced to achieve hover was formulated using this data.

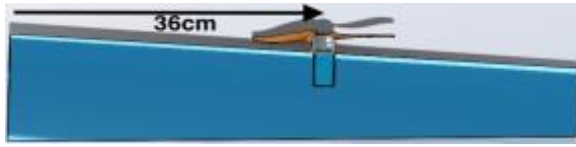


Figure 2a). Motor and propeller in configuration 1.



Figure 2b). Motor and propeller in configuration 2.

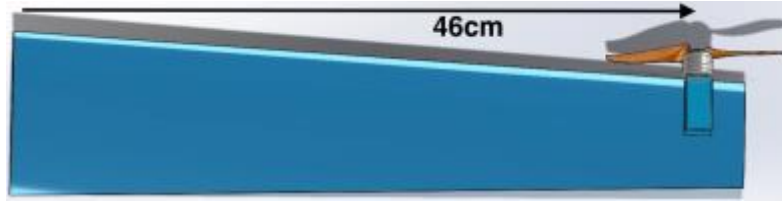


Figure 2c). Motor and propeller in configuration 3.

III. Results and Discussion

A. Calibration Curve

With the use of MATLAB®, the following plot was obtained:

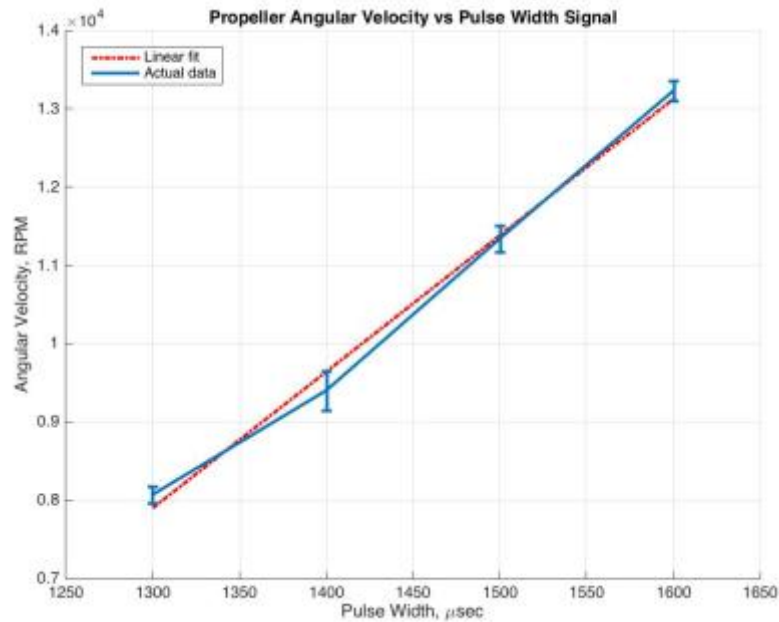


Figure 3. Propeller angular velocity as a function of pulse width signal.

The specific propeller used for the rotorcraft produced a minimum angular velocity of 8070 RPM and a maximum angular velocity of 13230 RPM. The data was fitted using a linear best fit line with equation

$$y = 17x - 14749 \quad (2)$$

Where, x is the pulse width signal in μs and y is the propeller speed in RPM

This equation was used to extract propeller angular velocities for given pulse width signals during the course of the experiment.

B. Early Predictions

As a method of checking the accuracy of the model used throughout the analysis, the angular velocity and the thrust produced by the propeller for each of the three configurations were predicted ahead of experimentation. These predictions were to be then compared with the actual values once the experiment was completed. The predicted values were obtained by firstly calculating the required thrust for hover using the following formula:

$$T_{prop} = \frac{Q}{R} \quad (3)$$

The rotor wing torque, $Q = 0.056 \text{ Nm}$, was obtained from the aerodynamic analysis of the rotorcraft. Next, the airspeed at the propeller location was calculated using the following expression:

$$V = R\Omega \quad (4)$$

The wing rotational rate, $\Omega = 35.20 \text{ rad/s}$, was also found through the aerodynamic analysis. Note that, in order to achieve hover conditions, the following inequality must be satisfied:

$$T_{AP} \geq T_{prop} \quad (5)$$

In lieu of this, with T_{prop} and V in hand, the APC propeller data was used to obtain expected angular velocities and produced thrusts. The results are tabulated below:

Table 1. Table of predicted angular velocities and produced thrusts.

	$R \text{ (m)}$	$T_{prop} \text{ (N)}$	$V \text{ (m/s)}$	$T_{AP} \text{ (N)}$	$n_{predicted} \text{ (RPM)}$
Configuration 1	0.36	0.156	12.7	0.667	11000
Configuration 2	0.41	0.136	14.4	0.294	10000
Configuration 3	0.46	0.122	16.2	0.133	10000

As can be seen, the trend of the thrust produced by the propeller to achieve hover decreases as the motor and propeller are moved outwards along the span. This is as expected. However, the angular velocity of the propeller remains constant as the motor and propeller are moved further than 41 cm from the root. This is inconsistent with expectation, as the thrust produced by the propeller is directly proportional to its angular velocity. This inconsistency may be due to the nature of the propeller data that was used to extract these values. The data provided by APC Propellers offers angular velocity data at increments of 1000 RPM. As a result of this, the angular velocity of the propeller may be predicted only to the nearest 1000th RPM, this resolution does not allow for an accurate prediction. This is possibly the reason why no change is seen between the angular velocities of the second and third configuration of the motor and propeller.

C. Experimental Findings

The rotorcraft was then placed on the test stand in all of its three different configurations and data was collected using the GetSAM program. The pulse width signals that were obtained during hover were used to calculate the angular velocity of the propeller by means of the calibration curve and equation (2). Once this was done, the advance ratio was then calculated using equation (1). These values, along with the thrust produced, as obtained from the APC Propellers data are tabulated in the table below:

Table 2. Table of experimental angular velocities and produced thrusts.

	Pulse width signal (μs)	$n_{actual} \text{ (RPM)}$	$J \left(\frac{1}{rev}\right)$	$T_{prop} \text{ (N)}$	$T_{AA} \text{ (N)}^*$
Configuration 1	1581	12128	0.079	0.156	1.63
Configuration 2	1528	11227	0.097	0.136	1.37
Configuration 3	1462	10105	0.120	0.122	1.11

* A linear relationship was assumed between angular velocity and produced thrust in the APC Propellers data. Hence, linear interpolation was used to obtain exact thrust values for the respective n_{actual} values.

Similar to the predicted data, these experimental results show that the thrust required by the propeller decreases as it is moved outwards along the wingspan. In addition to this, the angular velocity of the propeller also decreases with an increase in spanwise location. This effect was not entirely captured in the earlier predictions. Furthermore, the availability of the ESC calibration curve throughout the experiment allowed for an accurate determination of the angular velocity. A plot of the thrust data obtained from the experiment can be seen in Fig. 4 below:

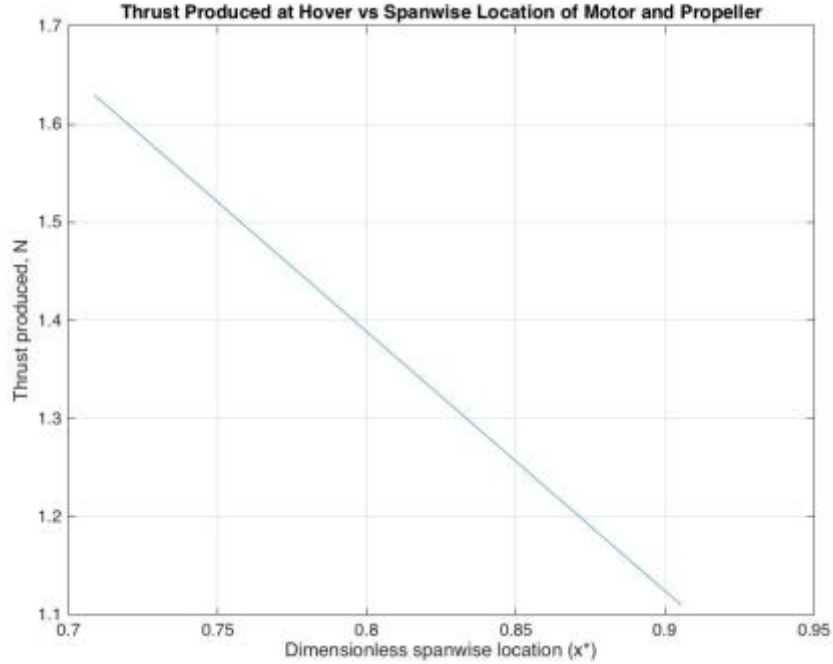


Figure 4. Variation of thrust as a function of spanwise location of motor and propeller.

Note that, x^* is the spanwise location normalized by the wingspan of the rotorcraft.

As expected, moving the motor and propeller outwards along the span of the rotorcraft's wing decreases the amount of thrust that is required to achieve hover. As a result, the propeller may rotate at lower angular velocities to produce this required thrust. However, it is important to note that there exists an approximately 1N difference between corresponding values of T_{AP} and T_{AA} . This systematic difference may most likely be attributed to the manner in which values of Q and Ω were obtained through numerical analysis. These parameters were calculated using values of $C_L(\alpha)$ and $C_D(\alpha)$ found through simulations in XFLR 5. The coefficients were obtained for a simulated NACA 2412 airfoil. In reality, the foam wing that was used contained many imperfections. For example, foreign adhesives and incisions were introduced on various parts of the wing. Considering this, it can be said that these imperfections were prominent enough to alter the values of $C_L(\alpha)$ and $C_D(\alpha)$ that were originally found through the simulation. Consequently, the parameters Q and Ω used in this analysis, which are dependent on these two coefficients were unrepresentative of the actual wing that was used.

IV. Conclusion

To conclude, the experimental findings show that moving the motor and propeller further outwards along the span of a single-blade rotorcraft reduced the amount of thrust that was required to achieve hover. The thrust produced varied in a linear fashion as motor and propeller location were manipulated. This reduction in thrust corresponded to a reduction in propeller angular velocity as well. This study has explicitly shown the relationship between motor and propeller location, and the resulting thrust that is produced to achieve hover. In addition, these findings have also provided the team with information that will allow for better decision making in the design of future single-blade rotorcraft.

References

¹ APC 5x3 propeller data, APC Propellers, Landing Products Inc.

² Dr. Mark Anderson, Department of Mechanical and Aerospace Engineering, University of California San Diego, La Jolla, CA